Fusion of Small Peroxisomal Vesicles In Vitro Reconstructs an Early Step in the In Vivo Multistep Peroxisome Assembly Pathway of *Yarrowia lipolytica*

Vladimir I. Titorenko, Honey Chan, and Richard A. Rachubinski

Department of Cell Biology, University of Alberta, Edmonton, Alberta T6G 2H7, Canada

Abstract. We have identified and purified six subforms of peroxisomes, designated P1 to P6, from the yeast, *Yarrowia lipolytica*. An analysis of trafficking of peroxisomal proteins in vivo suggests the existence of a multistep peroxisome assembly pathway in *Y. lipolytica*. This pathway operates by conversion of peroxisomal subforms in the direction P1, P2→P3→P4→P5→P6 and involves the import of various peroxisomal proteins into distinct vesicular intermediates. We have also reconstituted in vitro the fusion of the earliest intermediates in the pathway, small peroxisomal vesicles P1 and P2. Their fusion leads to the formation of a larger and more dense peroxisomal vesicle, P3. Fusion of P1 and P2 in vitro requires cytosol and ATP hydrolysis and is inhibited by antibodies to two membrane-associated ATPases of the AAA family, Pex1p and Pex6p. We provide evidence that the fusion in vitro of P1 and P2 peroxisomes reconstructs an actual early step in the peroxisome assembly pathway operating in vivo in *Y. lipolytica*.

Key words: microbody • peroxisomal protein import • biogenesis • membrane fusion • in vitro reconstitution

Introduction

The dynamic balance between fission and fusion of organelle membranes regulates organelle assembly and inheritance (Rothman and Warren, 1994; Warren and Wickner, 1996). To characterize the machinery of membrane fusion, homotypic (self) fusion reactions for different organelles have been reconstituted in vitro (Denesvre and Malhotra, 1996; Warren and Wickner, 1996). Comparative analyses of homotypic membrane fusion and of heterotypic (vectorial) vesicle-to-organelle membrane fusion have revealed wide variation in the spectra, topology, and regulation of components mediating membrane fusion.

Most heterotypic fusion reactions in the secretory pathway depend on the cytosolic factors *N*-ethylmaleimide-sensitive factor (NSF)[1] and soluble NSF attachment proteins (SNAPs; Rothman, 1994; Pfeffer, 1996). Heterotypic fusion of secretory vesicles to their target membranes is initiated by binding of SNAP receptors (SNAREs), which are vesicle- and target-specific integral membrane proteins (v-SNAREs and t-SNAREs, respectively; Rothman, 1994). Recruitment of NSF and SNAPs to the complex formed by v- and t-SNAREs yields the SNARE complex (Rothman, 1994). According to the SNARE hypothesis (Rothman, 1994), ATP hydrolysis by NSF causes disassembly of the SNARE complex and drives heterotypic membrane fusion. Recently, it has been reported that NSF and SNAPs may act at an ATP-dependent perfusion step rather than in heterotypic membrane fusion itself (Chamberlain et al., 1995; Banerjee et al., 1996; Otto et al., 1997; Weber et al., 1998).

Homotypic fusion of yeast vacuoles requires Sec18p (NSF) and Sec17p (the yeast α-SNAP homologue; Haas and Wickner, 1996). ATP hydrolysis by Sec18p drives Sec17p release, disassembly of unproductive interactions between v- and t-SNAREs on the same membrane, and activation of t-SNAREs (Nichols et al., 1997; Ungermann et al., 1998; Ungermann and Wickner, 1998). All these rearrangements occur at a vacuole priming step that precedes docking and fusion steps. Homotypic fusion of ER membranes in yeast is Sec18p- and Sec17p-independent (Latterich and Schekman, 1994) and is instead mediated by Cdc48p, another NSF-like AAA family ATPase (Latterich et al., 1995; Patel and Latterich, 1998). Reassembly of Golgi cisternae from drug-induced and postmitotic frag-

Address correspondence to Richard A. Rachubinski, Department of Cell Biology, University of Alberta, Medical Sciences Building 5-14, Edmonton, Alberta T6G 2H7, Canada. Tel.: (780) 492-9868. Fax: (780) 492-9278. E-mail: rick.rachubinski@ualberta.ca

[1]*Abbreviations used in this paper:* AOX, acyl-CoA oxidase; HSP, high-speed pelletable peroxisomes; NSF, *N*-ethylmaleimide-sensitive factor; SNAPs, soluble NSF attachment proteins; SNAREs, SNAP receptors; v-SNAREs and t-SNAREs, vesicle- and target-specific integral membrane proteins, respectively.

ments is mediated by NSF and the AAA family ATPase, p97/VCP (Acharya et al., 1995; Rabouille et al., 1995).

Recent findings have pointed to the possibility of membrane fusion acting in the assembly of peroxisomes. Two proteins essential for peroxisome biogenesis, the peroxins Pex1p and Pex6p, are ATPases of the AAA family (Erdmann et al., 1991; Faber et al., 1998; Titorenko and Rachubinski, 1998), members of which are required for all known homotypic and heterotypic membrane fusions (Patel and Latterich, 1998). Deficiency in Pex1p and Pex6p results in the accumulation of small peroxisomal vesicles in the yeasts, *Pichia pastoris* (Spong and Subramani, 1993; Heyman et al., 1994), *Saccharomyces cerevisiae* (Purdue and Lazarow, 1995), and *Yarrowia lipolytica* (Titorenko and Rachubinski, 1998), and in CHO (Tamura et al., 1998) and human cells (Geisbrecht et al., 1998; Tamura et al., 1998), suggesting a defect in vesicle fusion during peroxisome assembly (Acharya et al., 1995; Faber et al., 1998; Subramani, 1998). In *P. pastoris*, Pex1p and Pex6p themselves have been shown to be associated with small peroxisomal vesicles that are distinct from mature peroxisomes (Faber et al., 1998). These vesicles have been proposed to undergo successive rounds of fusion to generate larger vesicles, which in turn could assemble the import machineries for peroxisomal membrane and matrix proteins, import these proteins from the cytosol, and eventually mature into large, functional peroxisomes (Subramani, 1996; Erdmann et al., 1997; Faber et al., 1998). Such a model predicts that peroxisome maturation might be a multistage process encompassing several consecutive steps and involving the import of various peroxisomal proteins into distinct intermediates. Evidence in support of this model comes from the demonstration that under certain conditions, the import of a subset of peroxisomal membrane proteins into early peroxisomal precursors might precede, and indeed be required for, the import of matrix proteins (South and Gould, 1999). These results satisfactorily explain numerous observations on the heterogeneity of mammalian and yeast peroxisomes in terms of their buoyant densities, protein compositions and import competencies (Heinemann and Just, 1992; Lüers et al., 1993; van Roermund et al., 1995; Wilcke et al., 1995; van der Klei and Veenhuis, 1996). It should be noted, however, that small peroxisomal vesicles, the postulated intermediates in the peroxisome assembly process, have not yet been identified, purified, or characterized. Furthermore, it remains unclear whether peroxisomal vesicles can actually fuse with one another, what type of peroxisome could be formed by fusion, and what might be the requirements of the fusion process itself, particularly in regards to the ATPases, Pex1p and Pex6p.

Here we report the identification and purification of six subforms of peroxisomes from *Y. lipolytica*. We show that these subforms are organized into a multistep peroxisome assembly pathway. This pathway operates by the directed conversion of different subforms and involves the import of various peroxisomal proteins into distinct intermediates along the pathway. We also reconstitute in vitro the fusion of two populations of small peroxisomal vesicles that represent the earliest intermediates in the assembly pathway. We provide evidence that the in vitro fusion reaction reconstructs an actual in vivo peroxisome assembly event that requires the action of the ATPases, Pex1p and Pex6p.

Materials and Methods

Strains and Reagents

The *Y. lipolytica* strains used in this study, media, growth conditions, and genetic techniques have been described (Eitzen et al., 1997; Titorenko et al., 1997). The specificities of anti-SKL antibodies and antibodies to acyl-CoA oxidase (AOX), thiolase (THI; Szilard et al., 1995); isocitrate lyase (ICL), malate synthase (MLS; Titorenko et al., 1998); Pex2p (Eitzen et al., 1996); Pex16p (Eitzen et al., 1997); Kar2p and Sec14p (Titorenko et al., 1997) have been described. Anti-AOX antibodies used in this study specifically recognize peroxisomal isoform Aox1p (data not presented), one of five AOXs in *Y. lipolytica* (Wang et al., 1999). Antibodies to Pex1p and Pex6p, which were raised against fusions of Pex1p and Pex6p with maltose-binding protein, specifically recognized 100- and 116-kD polypeptides, respectively, in cell lysates of the wild-type strain but not in lysates of the *pex1KO* and *pex6KO* mutant strains (data not presented). The nucleotide sequence of the *Y. lipolytica PEX1* gene and the deduced amino acid sequence of its encoded protein, Pex1p, have been deposited in the DDBJ/EMBL/GenBank databases with accession number AF208231. Fab fragments of IgGs were produced using the ImmunoPure Fab Preparation Kit (Pierce), followed by Fab concentration and buffer exchange (Haas and Wickner, 1996).

Subcellular Fractionation and Peroxisome Isolation

Subcellular fractionation of *Y. lipolytica* cells grown in oleic acid-containing YPBO medium and isolation of highly purified mature peroxisomes, P6, were performed as described previously (Titorenko et al., 1998). To purify different subforms of high-speed pelletable peroxisomes (HSP), a 200,000-*g* pellet fraction (200KgP) was subjected to centrifugation on a discontinuous sucrose (18, 25, 30, 35, 40, and 53%, wt/wt) gradient at 120,000 *g* for 18 h at 4°C in a Beckman SW28 rotor. 36 fractions of 1 ml each were collected. Fractions containing different subforms of HSP were recovered, and 4 vol of 0.5 M sucrose in buffer H (5 mM MES, pH 5.5, 1 mM KCl, 0.5 mM EDTA, 0.1% ethanol, and a mixture of protease inhibitors; Szilard et al., 1995) were added. Peroxisomes were pelleted onto a 150-μl cushion of 2 M sucrose in buffer H by centrifugation at 200,000 *g* for 20 min at 4°C in a Beckman TLA120.2 rotor. Individual pellets of different subforms of HSP were resuspended in 3 ml of 50% (wt/wt) sucrose in buffer H.

For purification of HSP subforms P1 and P2, pellets of P1 and P2 resuspended in 50% (wt/wt) sucrose in buffer H were overlaid with 30, 28, 26, 24, 22, and 10% sucrose (all wt/wt in buffer H). After centrifugation at 120,000 *g* for 18 h at 4°C in a SW28 rotor, 18 fractions of 2 ml each were collected. P1 and P2 were pelleted, resuspended and subjected to a second flotation on the same multistep sucrose gradient. Gradients were fractionated into 2-ml fractions as above, and P1 and P2 were recovered and pelleted. Pelleted P1 and P2 were resuspended in T99 buffer (15 mM MES, pH 6.0, 100 mM KCl, 50 mM KOAc, 3 mM $MgCl_2$, 2 mM MgOAc) containing 250 mM sorbitol, and washed twice by resuspension in this buffer containing sorbitol followed by centrifugation, as described above. P1 and P2 were ultimately resuspended in T99 buffer plus 250 mM sorbitol and used in the fusion assay.

For purification of HSP subforms P3 and P4, pellets of P3 and P4 resuspended in 50% (wt/wt) sucrose in buffer H were overlaid with 38%, 35%, 33% and 20% sucrose (all wt/wt in buffer H). After centrifugation at 120,000 *g* for 18 h at 4°C in a SW28 rotor, 18 fractions of 2 ml each were collected. P3 and P4 were pelleted, resuspended in 3 ml of 50% (wt/wt) sucrose in buffer HE (20 mM MES, pH 5.5, 20 mM EDTA, 0.1% ethanol), overlaid with 39, 37, 35, 33, and 20% sucrose (all wt/wt in buffer HE), and subjected to centrifugation as above. Gradients were fractionated into 2-ml fractions, and P3 and P4 were recovered and pelleted. After resuspension in 3 ml of 50% (wt/wt) sucrose in buffer H, P3 and P4 were again subjected to flotation on the second multistep sucrose gradient described above. Gradients were fractionated into 2-ml fractions, and P3 and P4 were recovered and pelleted.

To recover peroxisomes from in vitro fusion reactions, reactions were placed on ice for 3 min and diluted 10-fold with ice-cold buffer H containing 250 mM sorbitol. Peroxisomes were pelleted, resuspended in 400 μl of 50% (wt/wt) sucrose in buffer H, overlaid with 30, 28, 26, 24, 22, and 10%

sucrose (all wt/wt in buffer H), and subjected to centrifugation at 200,000 *g* for 18 h at 4°C in a Beckman SW50.1 rotor. 18 fractions of 275 μl each were collected.

Cytosol for in vitro peroxisome fusion reactions was prepared in T99 buffer containing 250 mM sorbitol, essentially as described (Rexach and Schekman, 1991).

In Vitro Peroxisome Fusion Assay

P1 were isolated from unlabeled wild-type, *pex5KO* or *pex16-HA* cells, while P2 were isolated from *pex5KO* cells labeled with L-[^{35}S]methionine for 30 min (Titorenko et al., 1998). The standard peroxisome fusion reaction (40 μl) contained 20 μg of unlabeled P1 and 20 μg of radiolabeled P2 in T99 buffer containing 250 mM sorbitol, 1 mg cytosol/ml, 1 mM ATP, 40 mM creatine phosphate, and 10 U creatine kinase/ml. The nonhydrolyzable analogues ATPγS and GTPγS were used at concentrations of 1 mM. After incubation at 26°C, reactions were placed on ice for 3 min and then diluted 10-fold with ice-cold D buffer (15 mM MES, pH 6.0, 250 mM sorbitol, and a cocktail of protease inhibitors). Peroxisomes were pelleted by centrifugation at 100,000 *g* for 8 min at 4°C in a TLA120.2 rotor, resuspended in 400 μl of D buffer, and repelleted. Immunoprecipitation of the precursor (pTHI) and mature (mTHI) forms of THI was performed under denaturing conditions (Titorenko et al., 1998) using anti-THI antibodies covalently coupled to protein A–Sepharose, as described (Xu et al., 1998). Immunoprecipitates were subjected to a second immunoprecipitation (recapture) step (Bonifacino and Dell'Angelica, 1998), resolved by SDS-PAGE, and visualized by fluorography. Fluorograms were quantitated by densitometry, and the percentage of conversion of pTHI to mTHI was calculated.

Other Methods

Pulse–chase experiments were performed as described (Titorenko et al., 1998). Activities of marker enzymes for peroxisomes, mitochondria, ER, Golgi, vacuole or plasma membrane were determined by established methods (Titorenko et al., 1998). Peroxisome lysis with Ti8 buffer (10 mM Tris-HCl, pH 8.0, 5 mM EDTA, 1 mM PMSF, and leupeptin, pepstatin, and aprotinin each at 1 μg/ml), protein extraction, and protease protection analysis of purified peroxisomes were performed as described (Szilard et al., 1995). Phospholipids were extracted from whole peroxisomes and quantitated as described (Matsuoka et al., 1995). SDS-PAGE and immunoblotting using a semi-dry electrophoretic transfer system were performed as described (Titorenko et al., 1998). Antigen-antibody complexes were detected by enhanced chemiluminescence (Amersham). Samples for EM analysis were sedimented at 100,000 *g* for 20 min at 4°C in a Beckman TLS55 rotor onto a bed (25–50 μl) of hardened, low-melting 2.5% NuSieve GTG agarose (FMC) and were further processed as described (Eitzen et al., 1997). Silver/gold thin sections through oriented pellets were analyzed.

Results

Purification and Characterization of Multiple Subforms of High-Speed Pelletable Peroxisomes

Yeast peroxisomes are usually isolated by isopycnic density gradient centrifugation of a low-speed (20,000 *g*) pelletable organellar fraction (20KgP; Aitchison et al., 1992). Recently, we have shown that peroxisomal matrix and membrane proteins of *Y. lipolytica* are associated not only with the 20KgP but also with a high-speed (200,000 *g*) pelletable fraction (200KgP; Titorenko et al., 1998). Analysis of the in vivo trafficking of peroxisomal proteins has revealed that high-speed pelletable peroxisomes (HSP) are precursors to mature, low-speed pelletable peroxisomes (LSP) recovered in the 20KgP (Titorenko et al., 1998). To purify HSP, we first fractionated the 200KgP by isopycnic centrifugation on a discontinuous sucrose density gradient. Four peaks of peroxisomal proteins at densities of 1.18

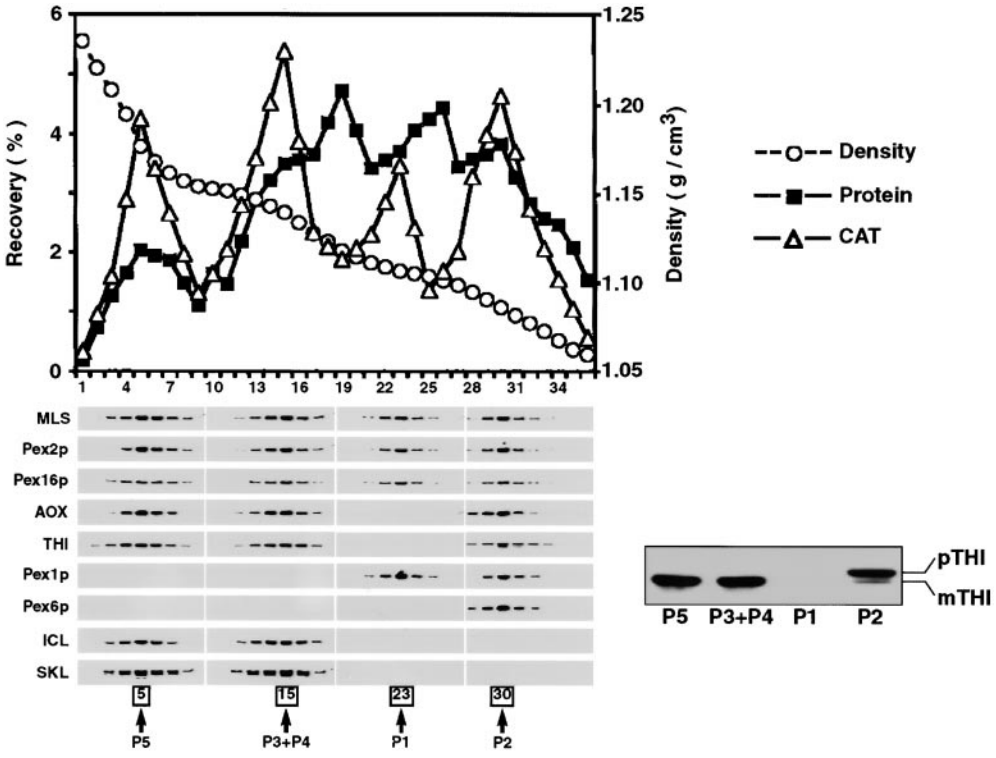

Figure 1. Separation of subforms of high-speed pelletable peroxisomes (HSP). The 200KgP fraction from the wild-type strain *E122* grown in YPBO for 9 h was fractionated by isopycnic centrifugation on a discontinuous sucrose gradient. Sucrose density (g/cm^3) of fractions and the percent recovery of loaded protein and of catalase (CAT) activity in fractions are presented. Fractions were analyzed by immunoblotting with antibodies to peroxisomal matrix (MLS, AOX, THI, ICL, and SKL) and membrane (Pex2p, Pex16p, Pex1p, and Pex6p) proteins. Numbers in boxes and arrows indicate the peak fractions for different subforms of HSP (P1, P2, P3+P4, and P5). These peak fractions (10 μg of protein) were immunodecorated with anti-THI antibodies. The positions of the 47-kD precursor form (pTHI) and of the 45-kD mature form (mTHI) of THI are indicated.

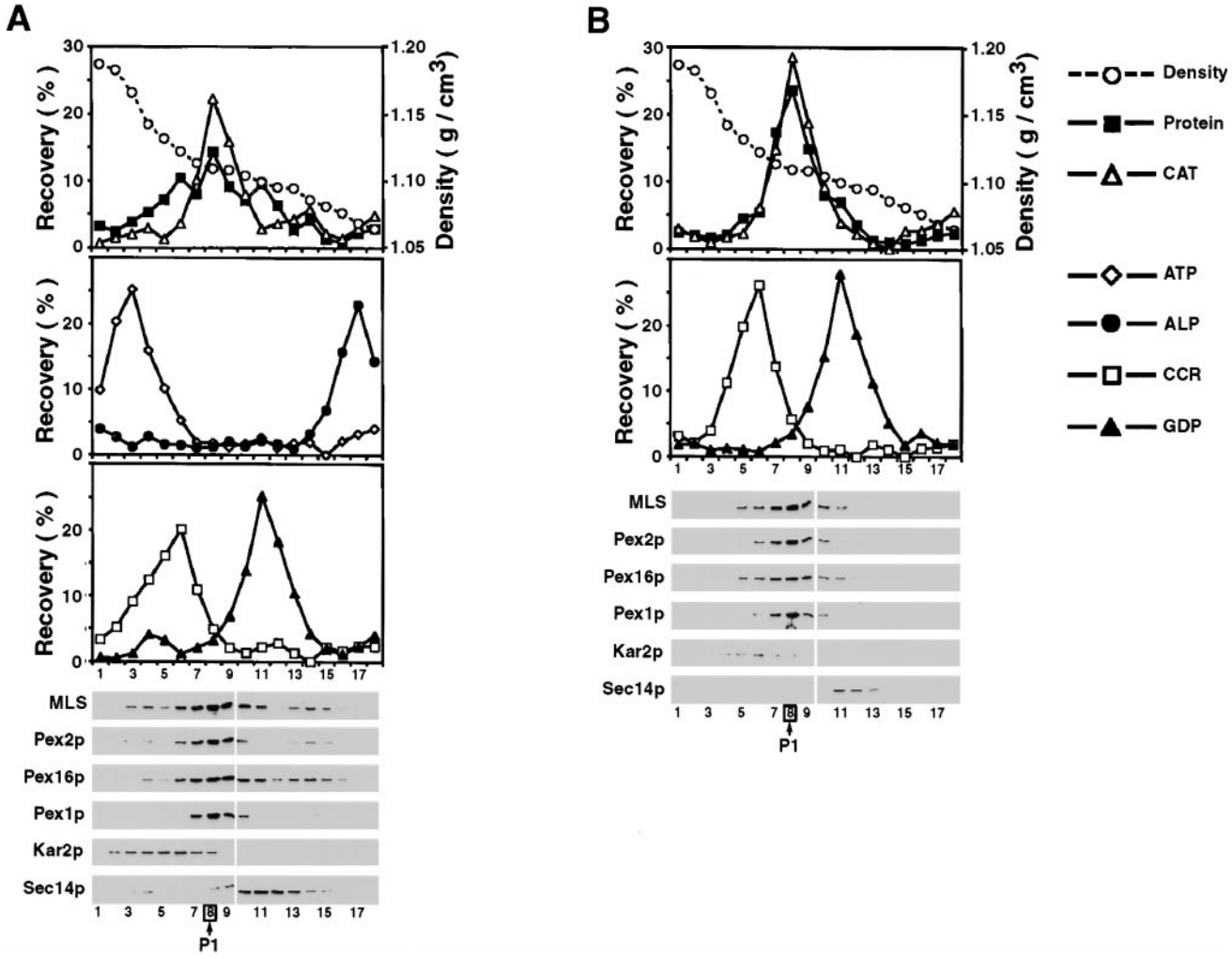

Figure 2. Purification of P1 peroxisomes. (A) Fractions 21 to 24 containing P1 peroxisomes recovered from the gradient reported in Fig. 1 were pooled and subjected to flotation to equilibrium on a multistep sucrose density gradient as described in Materials and Methods. (B) The peak fractions containing P1 peroxisomes recovered from the gradient reported in A were pooled and brought to equilibrium by flotation on a second sucrose density gradient as described in Materials and Methods. Fractions in A and B were analyzed for sucrose density (g/cm^3); for the percent recoveries of loaded protein and of CAT (peroxisome), alkaline phosphatase (ALP; vacuole), vanadate-sensitive ATPase (ATP; plasma membrane), NADPH/cytochrome *c* reductase (CCR; ER) and guanosine diphosphatase (GDP; Golgi) marker enzyme activities; and by immunoblotting to peroxisomal matrix (MLS) and membrane (Pex2p, Pex16p, and Pex1p) proteins and to Kar2p (ER) and Sec14p (Golgi) protein markers. (C) Electron micrographs of an oriented pellet preparation of purified P1 peroxisomes. Panels show two magnifications of the same micrograph. Bars, 0.2 μm.

g/cm^3 (fraction 5, P5), 1.14 g/cm^3 (fraction 15, P3+P4), 1.11 g/cm^3 (fraction 23, P1), and 1.09 g/cm^3 (fraction 30, P2) were recovered (Fig. 1). Catalase activity detected in fractions 9, 18, and 27, which was ~25–50% of the activity recovered in the four peak fractions of peroxisomal proteins, may have been the result of preferential leakage of catalase from peroxisomes during their isolation by subcellular fractionation (Roggenkamp et al., 1975). All per-

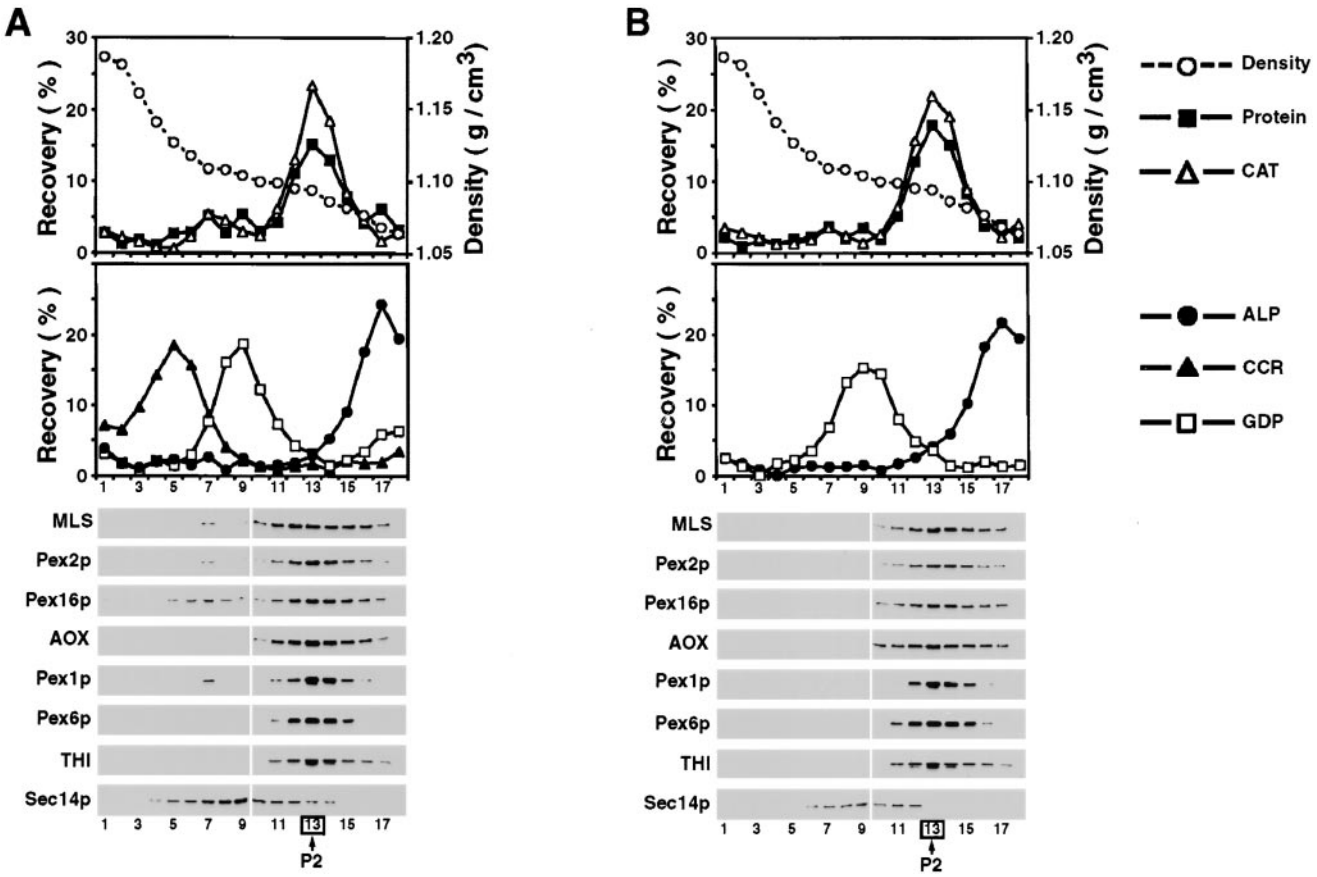

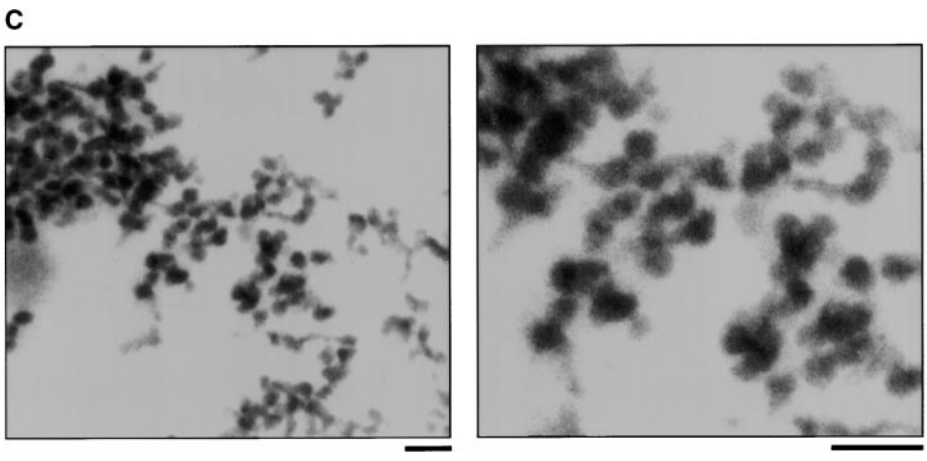

Figure 3. Purification of P2 peroxisomes. (A) Fractions 28–32 containing P2 peroxisomes recovered from the gradient reported in Fig. 1 were pooled and subjected to flotation to equilibrium on a multistep sucrose density gradient as described in Materials and Methods. (B) The peak fractions containing P2 peroxisomes recovered from the gradient reported in A were pooled and brought to equilibrium by flotation on a second sucrose gradient as described in Materials and Methods. Fractions in A and B were analyzed as described in the legend to Fig. 2. (C) Electron micrographs of an oriented pellet preparation of purified P2 peroxisomes. Panels show two magnifications of the same micrograph. Bars, 0.2 μm.

oxisomal proteins recovered in peaks P1 (Fig. 2 A), P2 (Fig. 3 A), P3+P4 (Fig. 4 A), and P5 (data not presented) could float out of the most dense sucrose during centrifugation to equilibrium in sucrose density gradients. Accordingly, these proteins were present in membrane-associated form rather than in aggregates. Furthermore, matrix proteins recovered in the four peaks were resistant to digestion by external protease, i.e., were present in membrane-enclosed form (see Fig. 7 for data on P1 and P2). Together these data demonstrate the existence of multiple subforms of HSP in *Y. lipolytica.*

HSP subforms were further purified by flotation to equilibrium on additional sucrose density gradients (see Materials and Methods). P1 peroxisomes thus purified were essentially free of contamination by plasma membrane and vacuolar elements and contained <5 and 2% contamination by ER and Golgi elements, respectively (Fig. 2, A and B). EM of purified P1 peroxisomes revealed a homoge-

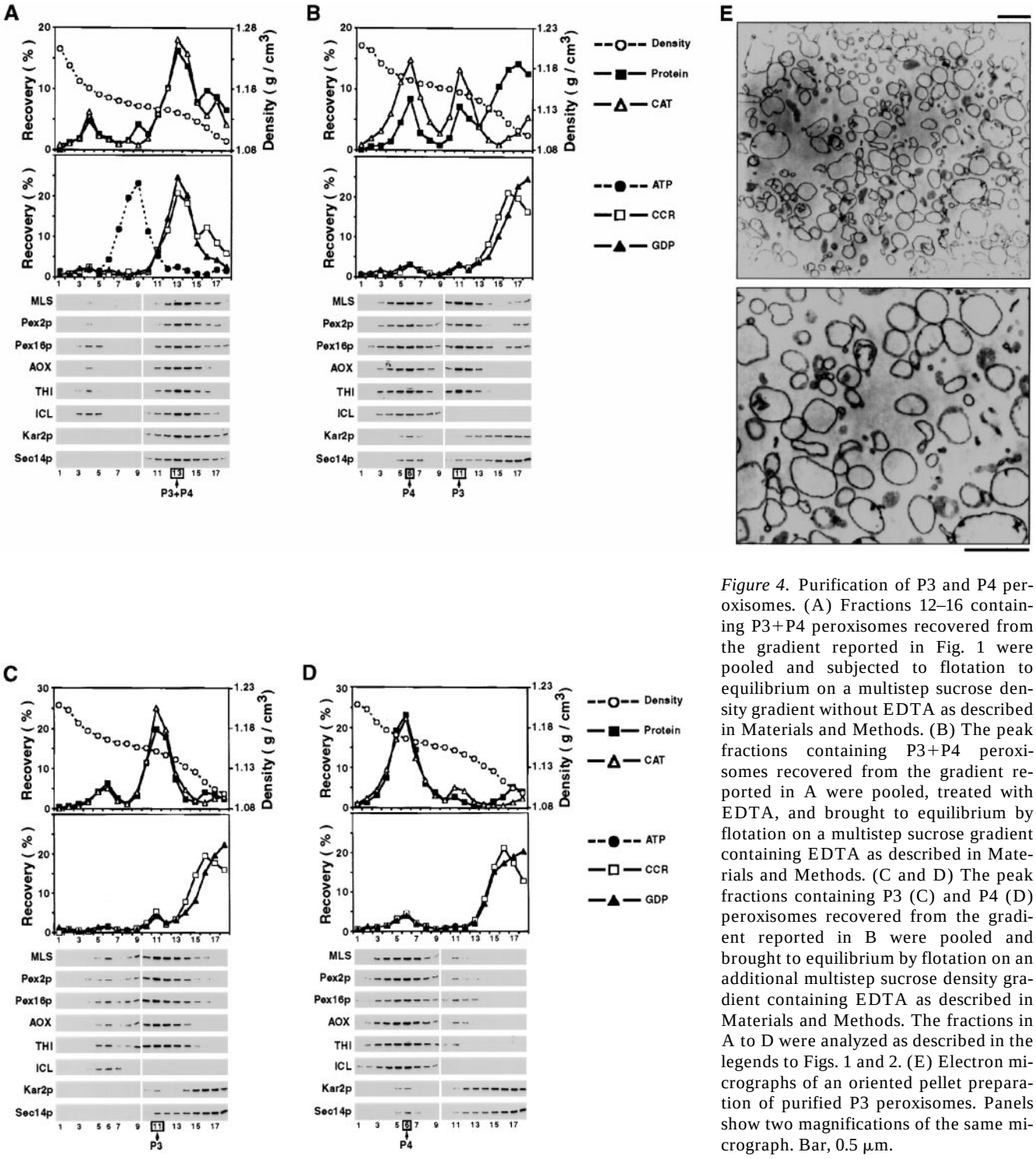

Figure 4. Purification of P3 and P4 peroxisomes. (A) Fractions 12–16 containing P3+P4 peroxisomes recovered from the gradient reported in Fig. 1 were pooled and subjected to flotation to equilibrium on a multistep sucrose density gradient without EDTA as described in Materials and Methods. (B) The peak fractions containing P3+P4 peroxisomes recovered from the gradient reported in A were pooled, treated with EDTA, and brought to equilibrium by flotation on a multistep sucrose gradient containing EDTA as described in Materials and Methods. (C and D) The peak fractions containing P3 (C) and P4 (D) peroxisomes recovered from the gradient reported in B were pooled and brought to equilibrium by flotation on an additional multistep sucrose density gradient containing EDTA as described in Materials and Methods. The fractions in A to D were analyzed as described in the legends to Figs. 1 and 2. (E) Electron micrographs of an oriented pellet preparation of purified P3 peroxisomes. Panels show two magnifications of the same micrograph. Bar, 0.5 μm.

nous population of vesicles 87 ± 8 nm in diameter (n = 250; Fig. 2 C). Purified P2 peroxisomes contained no detectable ER contamination and <2% contamination by Golgi and vacuolar elements (Fig. 3, A and B). EM of purified P2 peroxisomes showed a uniform population of vesicles 81 ± 11 nm in diameter (n = 250; Fig. 3 C).

Approximately 20% of total ER markers and 20% of total Golgi markers recovered during isopycnic centrifugation of the 200KgP cofractionated with peroxisomes comprising peak P3+P4 (data not presented). These ER and Golgi elements could not be separated from P3+P4 during flotation to equilibrium on a sucrose density gradient (Fig. 4 A). However, treatment of P3+P4 with EDTA, followed by flotation on a sucrose density gradient containing EDTA (see Materials and Methods), led to the separation of ER and Golgi elements from peroxisomal elements (Fig. 4 B). Two peroxisomal subforms were recovered, one (P3) peaking at a density of 1.15 g/cm^3 (Fig. 4 B, fraction

11) and a second (P4) peaking at a density of 1.17 g/cm^3 (Fig. 4 B, fraction 6). These two subforms represent two distinct types of HSP rather than arise artefactually in vitro by EDTA-stimulated fragmentation of a single ancestor, because while both P3 and P4 contain MLS, AOX, THI, Pex2p, and Pex16p, only P4 contains ICL (Fig. 4 B). The dissociation of two distinct peroxisomal subforms from specific elements of the ER and Golgi by EDTA has previously been reported for peroxisome-deficient *pex2* mutants (Titorenko et al., 1996). Further purification on additional equilibrium flotation gradients (see Materials and Methods) yielded P3 and P4 peroxisomes free of contamination by plasma membrane and vacuolar elements and containing no more than 4–6% contamination by ER and Golgi elements (Fig. 4, C and D). EM of purified P3 peroxisomes revealed vesicles 288 ± 57 nm in diameter (n = 300; Fig. 4 E).

Quantitative immunoblot analysis of MLS and measurement of the enzymatic activity of CAT were used to determine the yield and percent recovery of individual forms of HSP and LSP. Typically, protein recovery from 1 L of wild-type cells grown in oleic acid–containing medium was 0.6 mg for P1, 0.8 mg for P2, 0.6 mg for P3, 0.7 mg for P4, 1.0 mg for P5, and 22.8 mg for mature LSP, P6. After final purification, the recoveries of individual forms of HSP were 10–14% that obtained after the first fractionation of the 200KgP by isopycnic centrifugation, as reported in Fig. 1.

Dynamics of Peroxisomal Subforms

The multiple subforms of HSP described above are not artefactually formed during fractionation. Evidence for the existence of HSP has come from in vivo studies showing that peroxisomal matrix proteins made in the cytosol traffic first to HSP and then to LSP (Titorenko et al., 1998). Therefore, HSP are precursors to LSP. Data presented in Figs. 1–4 also show that the subforms of HSP are not artefactually formed by fragmentation of a singular HSP form during fractionation, as the different subforms of HSP contain different combinations of peroxisomal proteins. All subforms contain the matrix proteins MLS and CAT and the membrane proteins Pex2p and Pex16p. P1 lacks the matrix proteins THI, AOX, anti-SKL–reactive proteins, and ICL. P2 lacks ICL and anti-SKL–reactive proteins, while P3 lacks ICL. In contrast, all these peroxisomal proteins are found in mature LSP, P6 (Titorenko et al., 1998). Pex6p is associated with P2, while Pex1p is found in P1 and P2, but not in P3, P4, or P5 (Fig. 1). Furthermore, P1 lacks THI, P2 contains mostly the 47-kD precursor of THI, pTHI, while P3, P4, and P5 accumulate only the 45-kD mature form of THI, mTHI (Fig. 1). Taken together, these data suggest two alternative mechanisms for the formation of LSP from HSP. In the first alternative, different subforms of HSP are unrelated, and each subform independently converts to mature peroxisomes through the import of a particular subset of peroxisomal proteins. In the second alternative, different subforms of HSP are related through the ordered conversion of one subform into another, resulting in an organized assembly pathway leading to the formation of mature LSP. To distinguish between these two alternatives, we studied the trafficking of peroxisomal proteins in vivo by pulse–chase analysis.

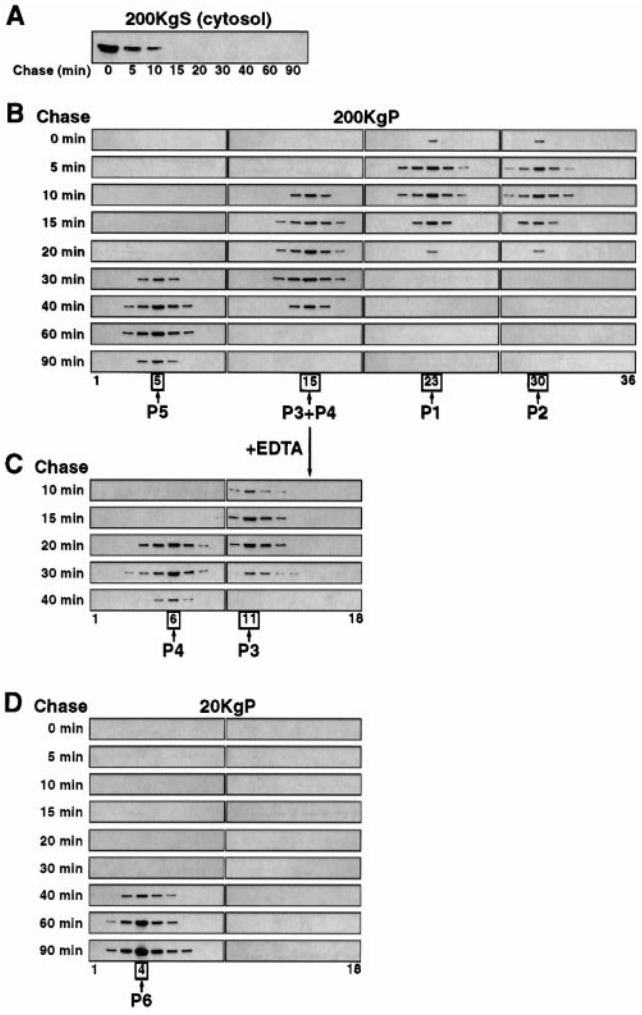

Figure 5. In vivo trafficking of the matrix protein, MLS. Spheroplasts of the wild-type strain *E122* grown in YPBO for 9 h were pulse-labeled for 1.5 min with L-[^{35}S]methionine and chased with unlabeled L-methionine. Samples were taken at the indicated times after chase. Spheroplasts were subjected to subcellular fractionation to yield 20KgP, 200KgP, and 200KgS (cytosol) fractions. The 20KgP (D) and 200KgP (B) fractions were further fractionated by isopycnic centrifugation on discontinuous sucrose density gradients. The combined P3+P4 peaks from the gradients reported in (B) were treated with EDTA and subjected to flotation analysis on sucrose density gradients containing EDTA to yield individual P3 and P4 peaks (C). MLS was immunoprecipitated from the cytosol and from individual fractions, and immunoprecipitates were resolved by SDS-PAGE and visualized by fluorography. Arrows indicate the peak fractions for P1 to P5 subforms of HSP and for mature LSP, P6.

The bulk of pulse-labeled MLS is initially found in the 200KgS (cytosolic) fraction, while small amounts are found in both P1 and P2 peroxisomes (compare Fig. 5, A and B). By 5 min, most MLS was chased from the cytosol to P1 and P2 (Fig. 5, A and B). From P1 and P2, MLS was chased to the P3+P4 peak, and by 30 min this transit was complete (Fig. 5 B). When P3 and P4 peroxisomes were separated from each other by treatment with EDTA, MLS

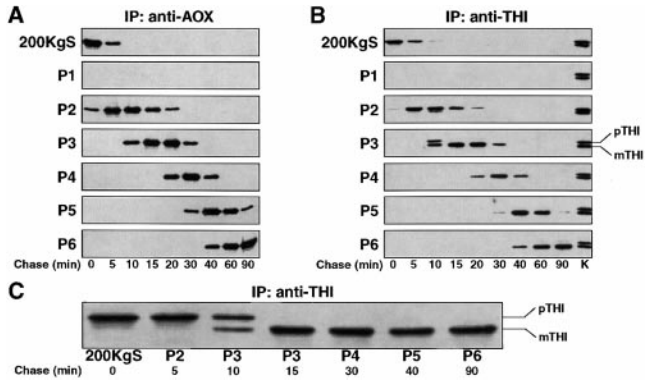

Figure 6. In vivo trafficking of the matrix proteins, AOX and THI. Spheroplasts of the wild-type strain *E122* were subjected to pulse–chase, subcellular fractionation, and immunoprecipitation with antibodies to AOX (A) and THI (B and C) as described in the legend to Fig. 5. Immunoprecipitates were resolved by SDS-PAGE and visualized by fluorography. The positions of the 47-kD precursor form (pTHI) and of the 45-kD mature form (mTHI) of THI are indicated. *K*, pTHI and mTHI immunoprecipitated from the peak fraction for P3 taken at 10 min of chase.

was seen to move from P1 and P2 to P3 (Fig. 5, B and C). By 20 min, MLS began to move from P3 to P4, and by 40 min this transfer was complete (Fig. 5 C). From P4, MLS was chased to P5 (Fig. 5 B), and from P5, MLS finally moved to mature LSP, P6 (Fig. 5, B and D). Together, these data show that different peroxisomal subforms convert in the direction P1, P2→P3→P4→P5→P6. This was further supported by an analysis of the in vivo trafficking of pulse-labeled AOX (Fig. 6 A) and THI (Fig. 6 B). In contrast to MLS, both AOX and THI initially chased from the cytosol to P2 only. There was no movement of AOX or THI from the cytosol to P1. Conversion of peroxisomal subforms as monitored by the chase of AOX and THI was in the direction P2→P3→P4→P5→P6. Notably, only pTHI was present in the cytosol (Fig. 6 C). Proteolytic maturation of pTHI to mTHI was negligible in P2 (Fig. 6, B and C). In contrast, pTHI that was chased from P2 to P3 was very quickly processed to mTHI (Fig. 6, B and C).

Development of an In Vitro Peroxisome Fusion Assay

The above data showing that MLS trafficked from the cytosol to both P1 and P2 and then to P3, while AOX and THI went from the cytosol to P2 alone and then to P3 are consistent with a scenario in which P3 is formed by fusion of P1 and P2. To test this hypothesis, we set about developing an in vitro assay for peroxisome fusion using P1 and P2. This assay is based on the proteolytic processing of a precursor form of a matrix protein, THI, to its mature form. In wild-type *Y. lipolytica* cells, the 47-kD precursor form of THI, pTHI, is synthesized in the cytosol and proteolytically processed to a 45-kD mature form, mTHI, after import into the matrix of HSP (Titorenko et al., 1998). Due to a defect in intraperoxisomal proteolytic processing, only pTHI is detected in peroxisomes of the peroxisome assembly mutant, *pex5KO* (Szilard et al., 1995). For an in vitro assay for peroxisome fusion, we mixed various combinations of P1 from unlabeled wild-type or *pex5KO* cells with P2 from L-[^{35}S]methionine-labeled *pex5KO* cells containing radiolabeled pTHI, and incubated them at 26°C in the presence or absence of cytosol from unlabeled wild-type cells, ATP, and an ATP-regenerating system. In the complete reaction (Fig. 7 A, lanes 1 and 2), up to 60% of pTHI was converted to mTHI. Several lines of evidence indicate that this maturation of pTHI was due to the fusion of P1 from wild-type cells with P2 from *pex5KO* cells, resulting in interaction of the pTHI-processing protease (from P1) with labeled pTHI (from P2) within the same compartment and proteolytic processing of pTHI to mTHI. First, incubation of P1 and P2 from the *pex5KO* strain under complete reaction conditions showed no formation of mTHI (Fig. 7 A, lane 3) because of the defect in intraperoxisomal proteolytic processing of pTHI observed for *pex5KO* peroxisomes. Second, solubilization of lumenal contents of P1 from wild-type cells and P2 from *pex5KO* cells by addition of detergent, followed by incubation in the absence of cytosol, ATP and an ATP-regenerating system, led to complete conversion of pTHI to mTHI (Fig. 7 A, lane 4). In contrast, no conversion was detected when P1 and P2 from the *pex5KO* strain were solubilized by detergent (Fig. 7 A, lane 5). Third, incubation of P2 from *pex5KO* cells in the presence of cytosol, ATP and an ATP-regenerating system, but in the absence of P1, showed no formation of mTHI (Fig. 7 A, lane 6). Therefore, proteolytic maturation of pTHI observed in the complete reaction was not due to the import of a processing protease into P2 from the cytosol or to breakage of P2 and cleavage of pTHI by cytosolic protease(s) during incubation. Fourth, no formation of mTHI was detected when cytosol, ATP and an ATP-regenerating system were omitted from the reaction (Fig. 7 A, lane 7). Therefore, proteolytic processing of pTHI in the complete reaction was not due to breakage of P1 and P2, with subsequent release of pTHI and the processing protease from broken peroxisomes.

Biochemical Requirements of Peroxisome Fusion In Vitro

Fusion of P1 and P2 in vitro requires cytosol (Fig. 7 B, compare lanes 1 and 3). Fusion was more efficient with cytosol from oleic acid-grown wild-type cells than with cytosol from glucose-grown cells (Fig. 7 B, compare lanes 1 and 2). Growth of *Y. lipolytica* in oleic acid–containing medium, but not in glucose-containing medium, requires assembly of functional peroxisomes and results in extensive peroxisome proliferation (Titorenko and Rachubinski, 1998). These data suggest that changes in the intracellular levels and/or the activity of cytosolic proteins required for peroxisome fusion are coordinated with growth substrate–dependent changes in peroxisome assembly and proliferation. Fusion of P1 and P2 in vitro requires ATP and an ATP-regenerating system (Fig. 7 B, compare lanes 1 and 4, and lanes 2 and 5). The use of ATP without an ATP-regenerating system resulted in fusion not more than 6–9% that observed in the complete reaction, while an ATP-regenerating system without ATP was unable to promote fusion (data not presented). These data suggest that fusion requires ATP hydrolysis. Indeed, no fusion was seen if the nonhydrolyzable analogue ATPγS

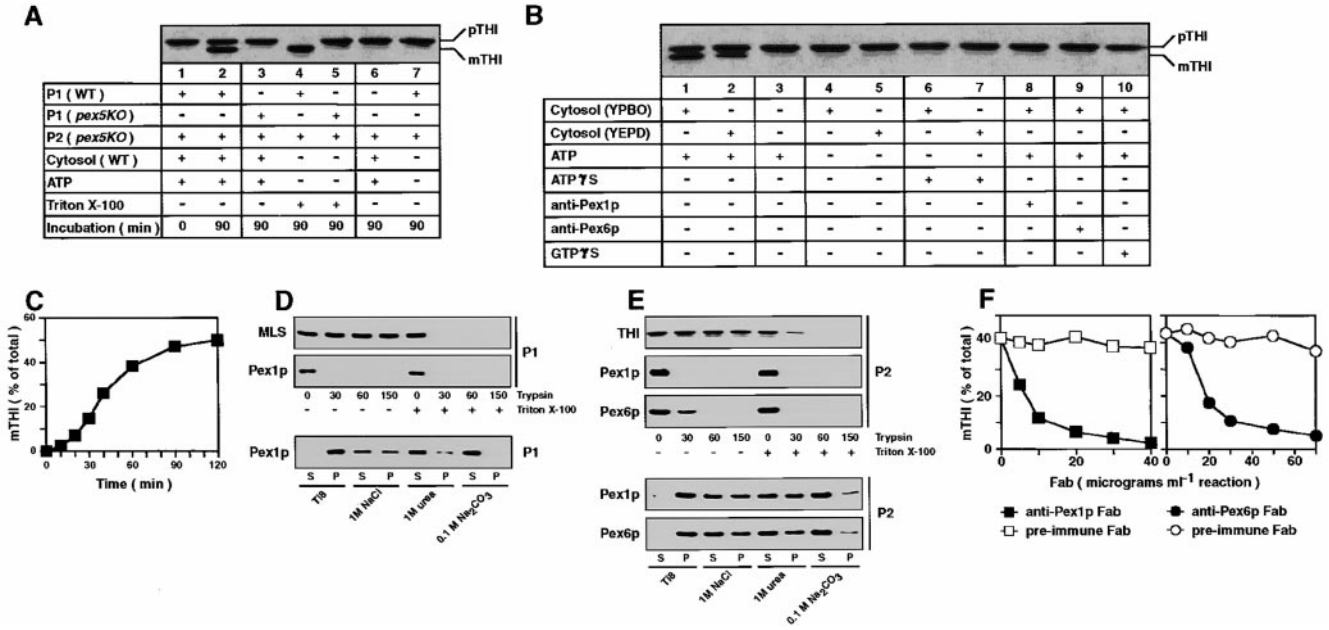

Figure 7. Requirements for peroxisome fusion in vitro. (A) P1 from unlabeled wild-type (WT) or *pex5KO* cells was mixed with P2 from *pex5KO* cells containing ^{35}S-labeled pTHI. Peroxisomes were incubated for the times indicated with or without cytosol from oleic acid (YPBO)-grown unlabeled wild-type cells, in the presence or absence of ATP, and with an ATP-regenerating system. Triton X-100 was added to 0.5% (vol/vol) to some samples. (B) P1 from unlabeled wild-type cells and P2 from *pex5KO* cells containing ^{35}S-labeled pTHI were combined and incubated for 90 min with or without cytosol from unlabeled oleic acid (YPBO)- or glucose (YEPD)-grown wild-type cells, in the presence or absence of ATP, ATPγS, GTPγS, anti-Pex1p (120 μg antibody/ml of reaction), or anti-Pex6p (250 μg antibody/ml of reaction), and with an ATP-regenerating system. (C) Aliquots of the complete fusion reaction were incubated at 26°C for the times indicated. Reactions in A–C were processed for immunoprecipitation of pTHI and mTHI, SDS-PAGE and fluorography. (A and E) For protease protection, P1 and P2 peroxisomes (30 μg of protein) were incubated with the indicated amounts (in μg) of trypsin in the absence or presence of 1.0% (vol/vol) Triton X-100 for 60 min on ice. Reactions were terminated by addition of TCA. Equal portions of the samples were analyzed by immunoblotting with the antibodies indicated. For organellar subfractionation, P1 and P2 peroxisomes were treated with one Ti8 buffer, 1 M NaCl, 1 M urea, or 0.1 M Na_2CO_3 (pH 11). After incubation on ice for 1 h, samples were separated into supernatant (S) and pellet (P) fractions by centrifugation and subjected to immunoblot analysis with antibodies to Pex1p (P1 and P2) and Pex6p (P2). (F) Effects of anti-Pex1p and anti-Pex6p Fab fragments on in vitro peroxisome fusion. Fab fragments from preimmune, anti-Pex1p or anti-Pex6p IgGs were mixed at the indicated concentrations with P1 from wild-type cells and P2 from *pex5KO* cells containing ^{35}S-labeled pTHI. Fusion reactions were started by addition of cytosol, ATP and an ATP-regenerating system. Reactions were transferred to 26°C and terminated after 90 min.

was used instead of ATP (Fig. 7 B, compare lanes 1 and 6, and lanes 2 and 7). None of ADP, UTP, GTP, GDP and CTP was able to promote peroxisome fusion in vitro (data not presented). Overall peroxisome fusion in vitro was inhibited by GTPγS (a nonhydrolyzable analogue of GTP) in the complete reaction, i.e., in the presence of cytosol and ATP (Fig. 7 B, compare lanes 1 and 10). Fusion of P1 and P2 in vitro had a lag period of ~10 min, was most rapid during the next 30–40 min, and reached steady state at levels of 50–60% processing of pTHI to mTHI after 90–120 min of incubation (Fig. 7 C). Fusion displayed a temperature optimum of 26°C and a pH optimum of 6.0 (data not presented).

Pex1p and Pex6p, NSF-like ATPases of the AAA Family, Are Required for Peroxisome Fusion In Vitro

Two AAA family ATPases, Pex1p and Pex6p, are required for peroxisome assembly in *Y. lipolytica* (Titorenko and Rachubinski, 1998). Pex1p and Pex6p have been suggested to be involved in vesicle fusion during peroxisome assembly in vivo (Acharya et al., 1995; Faber et al., 1998). In wild-type *Y. lipolytica* cells, Pex1p was associated with both P1 and P2, while Pex6p localized to P2 only (Fig. 1). The P1-associated form of Pex1p and the P2-associated forms of Pex1p and Pex6p were sensitive to externally added protease even in the absence of detergent, while the matrix proteins MLS and THI were degraded by trypsin only when P1 and P2 were disrupted by detergent (Fig. 7, D and E). The P1-associated form of Pex1p and the P2-associated forms of Pex1p and Pex6p were solubilized to a significant extent by 1 M NaCl or 1 M urea and completely by 0.1 M Na_2CO_3 (pH 11; Fig. 7, D and E). Therefore, Pex1p and Pex6p associate as peripheral membrane proteins with the cytosolic surface of P1 (Pex1p) and P2 (both proteins).

Overall fusion of P1 and P2 was inhibited by anti-Pex1p and anti-Pex6p antibodies (Fig. 7 B, lanes 8 and 9, respectively), while neither corresponding preimmune serum nor antibodies to matrix proteins affected fusion (data not presented). To avoid potential cross-linking of Pex1p or Pex6p by antibodies, we tested how monovalent Fab fragments prepared from anti-Pex1p and anti-Pex6p IgGs affected overall peroxisome fusion in vitro. Anti-Pex1p Fab

and anti-Pex6p Fab, but not Fab fragments from the corresponding preimmune sera, inhibited peroxisome fusion (Fig. 7 F). Therefore, in vitro fusion of P1 and P2 requires the two AAA ATPases, Pex1p and Pex6p.

In Vitro Fusion of P1 and P2 Peroxisomes Results in the Formation of Larger and More Dense P3 Peroxisomes

In the in vitro fusion assay, the extent of proteolytic processing of pTHI to mTHI is directly proportional to the number of fused peroxisomes and is used to quantitate peroxisome fusion. To apply independent criteria for peroxisome fusion and to test for potential changes in size, shape and/or morphology of fused peroxisomes, we used P1 from unlabeled *pex16-HA* cells and P2 from radiolabeled *pex5KO* cells containing ^{35}S-labeled pTHI. Instead of the wild-type form of the peroxisomal membrane protein Pex16p, P1 from *pex16-HA* cells contain Pex16p-HA, a modified Pex16p containing two copies of the hemagglutinin (HA) epitope at its carboxyl terminus (Eitzen et al., 1997). P1 from *pex16-HA* cells and P2 from *pex5KO* cells were mixed and incubated in the fusion reaction. Aliquots were taken 10 min and 90 min after the start of the reaction and subjected to fractionation by flotation on a multistep sucrose gradient. For the 0 min time point, aliquots of P1 and P2 were kept individually on ice and mixed immediately before fractionation. Fractionation of the 0 min time point revealed that the protein markers of P1 (Pex1p and Pex16p-HA) and P2 (Pex1p, Pex6p, and pTHI) floated out of the most dense sucrose and concentrated at densities of 1.11 g/cm^3 and 1.09 g/cm^3 for P1 and P2, respectively (Fig. 8 A). Protein markers remained specifically associated with P1 and P2, and therefore, the integrity of these peroxisomal subforms was not compromised during flotation. EM of oriented pellet preparations of peak fractions 8 and 14 revealed homogenous populations of small electron dense vesicles of average diameters 84 ± 10 nm and 88 ± 14 nm (n = 250) for P1 and P2, respectively (Figs. 9 B and 10 D).

Peroxisomes isolated after 10 min of the fusion reaction were predominantly of density 1.10 g/cm^3 and peaked in fraction 11 (Fig. 8 B). This form was designated P1/P2. Protein markers of P1 (Pex16p-HA) and P2 (pTHI) were recovered with the P1/P2 form (Fig. 8 B). No detectable Pex6p and only minor amounts of Pex1p were recovered with P1/P2 (compare Fig. 8, A and B), consistent with the observation that incubation of P1 and P2 in the fusion reaction results in the release of most Pex1p and Pex6p from the peroxisomal membrane (Titorenko and Rachubinski, manuscript in preparation). Only pTHI was recovered with P1/P2 (Fig. 8 D), demonstrating that the pTHI processing protease from P1 and pTHI from P2 were not localized within the same compartment. These data strongly suggest that the P1/P2 form represents a complex of docked, but unfused, P1 and P2 peroxisomes. This was borne out by EM analysis of P1/P2, which showed clustering of closely apposed peroxisomal vesicles of average diameter 75–100 nm like that of individual P1 and P2 peroxisomes (Fig. 9 B).

Two peroxisomal forms were present in the sample taken after 90 min of incubation. The P1/P2 form was still present (Figs. 8, C and D, and 9 B), as was a second form that peaked in fraction 4 and was more dense, 1.14 g/cm^3, than P1, P2 or P1/P2 (Fig. 8 C). This abundant form was designated P3. P3 accumulated Pex16p-HA (marker of P1) and THI (marker of P2; Fig. 8 C), which was only in its mature form, mTHI (Fig. 8 D). Therefore, the P3 form represents the product of fusion between P1 and P2. EM revealed that P3 had an average diameter of 269 ± 68 nm

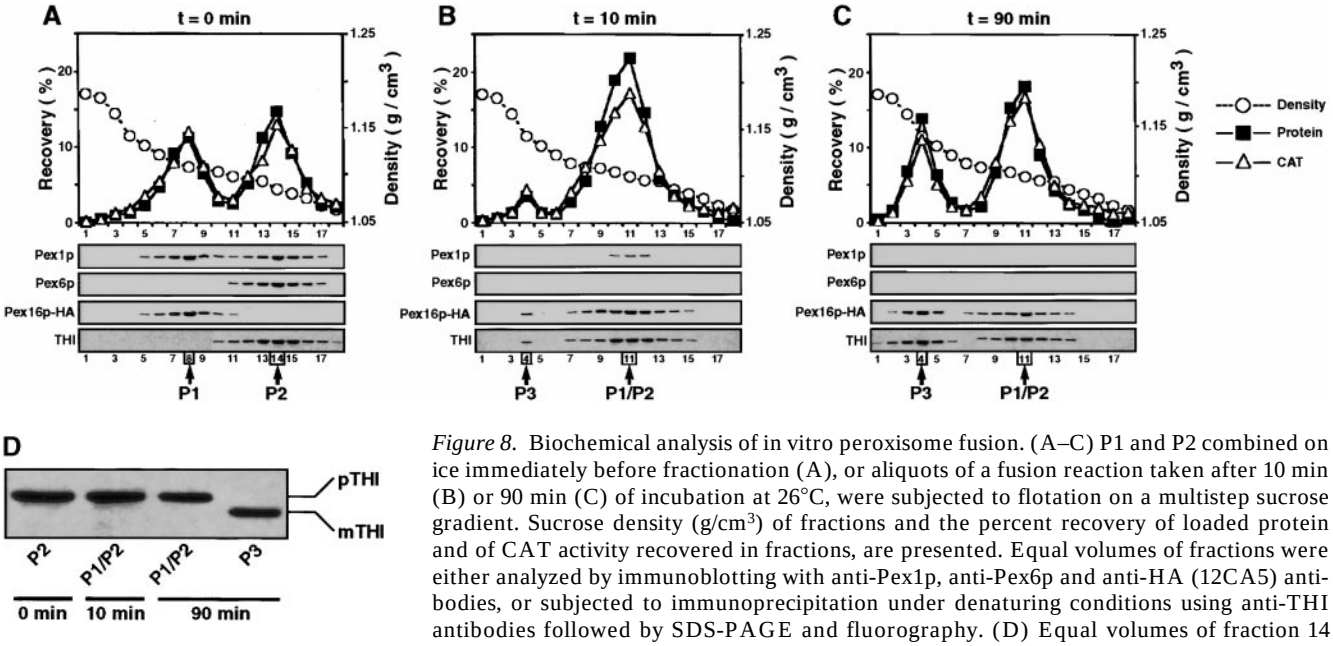

Figure 8. Biochemical analysis of in vitro peroxisome fusion. (A–C) P1 and P2 combined on ice immediately before fractionation (A), or aliquots of a fusion reaction taken after 10 min (B) or 90 min (C) of incubation at 26°C, were subjected to flotation on a multistep sucrose gradient. Sucrose density (g/cm^3) of fractions and the percent recovery of loaded protein and of CAT activity recovered in fractions, are presented. Equal volumes of fractions were either analyzed by immunoblotting with anti-Pex1p, anti-Pex6p and anti-HA (12CA5) antibodies, or subjected to immunoprecipitation under denaturing conditions using anti-THI antibodies followed by SDS-PAGE and fluorography. (D) Equal volumes of fraction 14 from gradient A (P2; 0 min), fraction 11 from gradient B (P1/P2; 10 min), and fractions 11 and 4 from gradient C (P1/P2 and P3, respectively; 90 min) were subjected to immunoprecipitation under denaturing conditions using anti-THI antibodies. Immunoprecipitates were resolved by SDS-PAGE and visualized by fluorography.

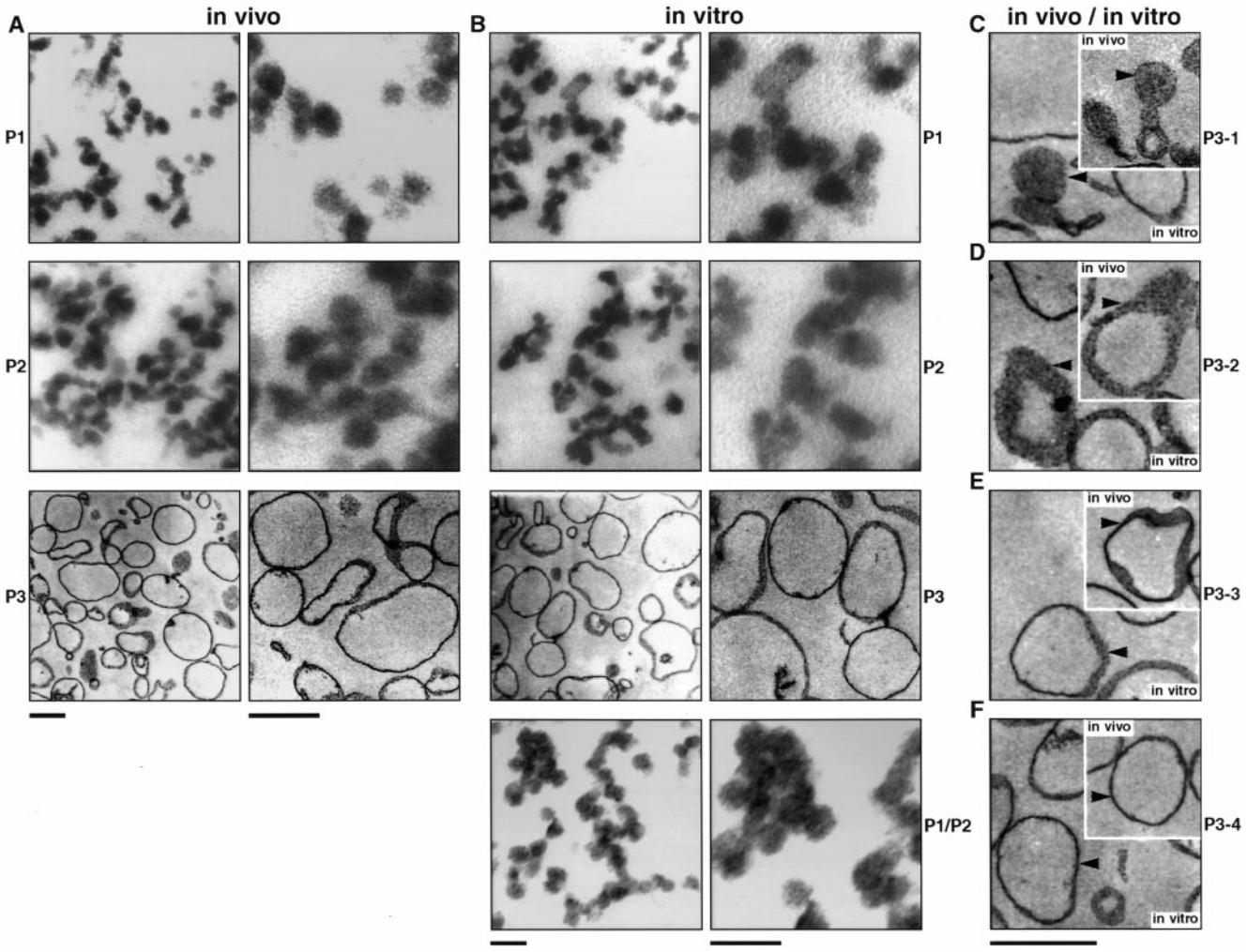

Figure 9. EM comparison of in vivo and in vitro peroxisomal subforms. (A, C–F) P1, P2, and P3 peroxisomes were purified from the 200KgP of YPBO-grown wild-type cells (in vivo). (B, C–F) P1, P2, and P3 peroxisomes and the P1/P2 docking complex were purified from a fusion reaction (in vitro) as presented in Fig. 9. P3-1, P3-2, P3-3, and P3-4 show different morphological types of P3 (see text). Bars, 0.2 μm.

(n = 300), roughly two to five times that of P1 or P2 (Figs. 9 B and 10 D). Four morphological types of in vitro formed P3 peroxisomes, designated P3-1, P3-2, P3-3, and P3-4, were observed (Fig. 9, C–F, respectively). The different types of P3 are discussed in greater detail below.

The buoyant density of P3 is greater than that of P1 or P2 (Fig. 8, A and C). Therefore, fusion of P1 and P2 yields a more dense peroxisome rather than an organelle of intermediate density. The reason for this remains obscure, but one can speculate that the buoyant density of any peroxisome depends on its size, shape, the total and relative levels of matrix and membrane proteins, the levels of (phospho)lipids and the (phospho)lipid/protein ratio. Fusion of P1 and P2 causes a significant change in size of the resulting organelle (Figs. 9 B and 10 D), while changes in other parameters are modest (Fig. 10). The cumulative effect of all these changes could result in higher buoyant density for P3 compared with P1 and P2.

Control experiments in which P1 and P2 were incubated individually in the fusion reaction did not show any morphological or biochemical evidence of fusion (data not presented). Therefore, neither P1 nor P2 is capable of self-fusion in vitro under conditions that support their inter-fusion.

Fusion of P1 and P2 Peroxisomes In Vitro Reconstructs an Early Step in Peroxisome Assembly In Vivo

We compared the biochemical and morphological properties of P1, P2, and P3 peroxisomes isolated from YPBO-grown wild-type cells (in vivo peroxisomes) to those of P1, P2, and P3 peroxisomes recovered from the in vitro peroxisome fusion reaction (in vitro peroxisomes). In vivo P1 peroxisomes were isolated from wild-type cells, while in vitro P1 originated from the *pex16-HA* strain. These two forms of P1 were very similar to each other in regards to buoyant density (1.11 g/cm^3 for both forms), size and morphology (Figs. 9, A and B, and 10 D), spectra of matrix (Fig. 10 A) and membrane (Fig. 10 B) proteins and their relative distributions (Fig. 10 E), levels of matrix and

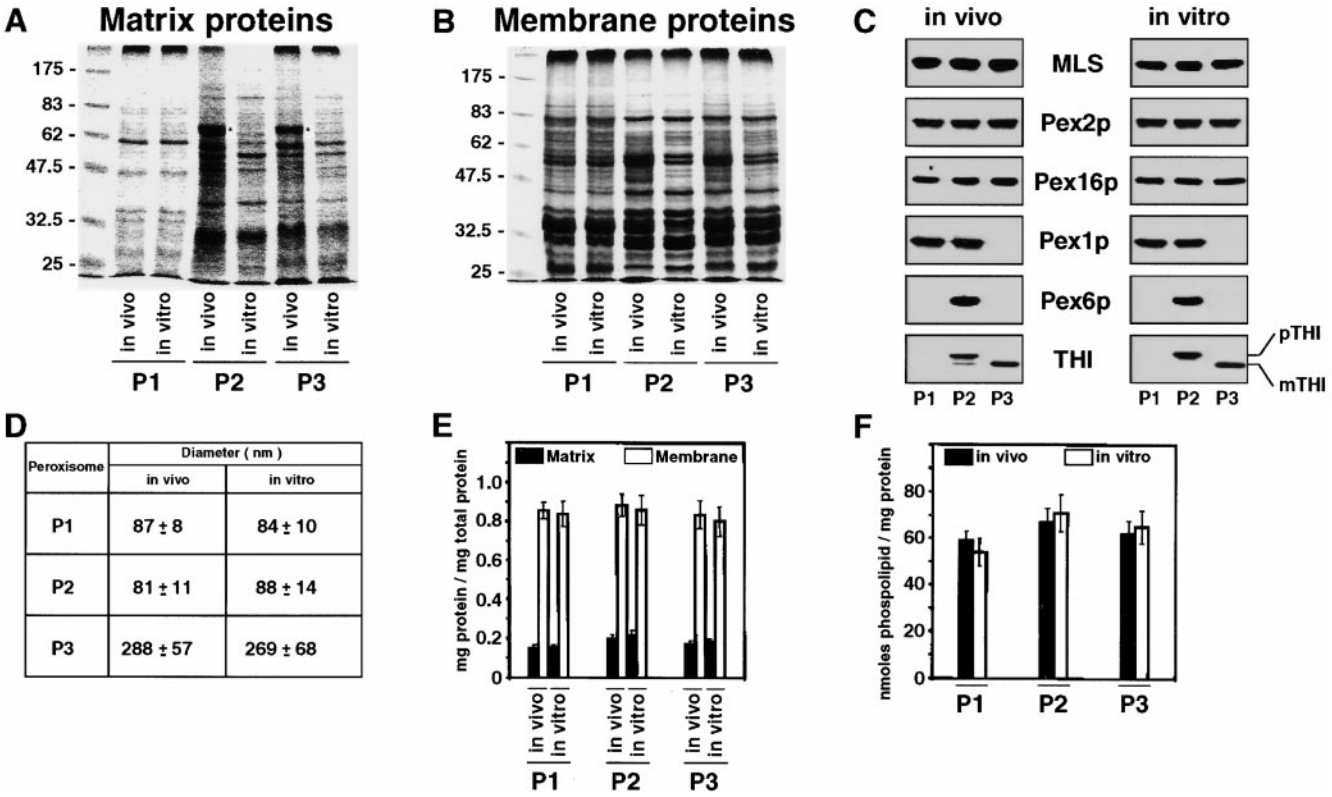

Peroxisome	Diameter (nm)	
	in vivo	in vitro
P1	87 ± 8	84 ± 10
P2	81 ± 11	88 ± 14
P3	288 ± 57	269 ± 68

Figure 10. Comparison of P1, P2, and P3 peroxisomes isolated from YPBO-grown wild-type cells (in vivo) or recovered from the in vitro fusion reaction (in vitro). The spectra of peroxisomal matrix (A) and membrane (B) proteins and their relative distributions (E), the levels of individual peroxisomal proteins (C), the size (D) and phospholipid/protein ratios (F) of in vivo and in vitro P1, P2, and P3 peroxisomes are presented. (A, B, and E) Purified peroxisomal forms (30 μg of protein) were lysed with Ti8 buffer and subjected to centrifugation to yield supernatant (matrix proteins) and pellet (membrane proteins) fractions. Recovered proteins were resolved by SDS-PAGE and stained with Coomassie Blue (A and B) or quantitated with a protein assay kit (E). The numbers at left in A and B indicate the migrations of molecular mass standards (in kD). (C) Equal quantities of protein from P1, P2, and P3 were analyzed by immunoblotting with antibodies to the proteins indicated. (D) Oriented pellet preparations of P1, P2, and P3 were fixed and processed for EM. The diameters of 250 (P1 and P2) or 300 (P3) structures were measured. (F) Phospholipid was extracted from P1, P2, and P3 and quantitated as described in Materials and Methods.

membrane proteins (Fig. 10 C) and phospholipid/protein ratios (Fig. 10 F).

In vivo P2 peroxisomes were purified from wild-type cells, while in vitro P2 were isolated from the *pex5KO* strain. The only distinction between these two forms was the absence of a 67-kD protein (Fig. 10 A, asterisk) in in vitro P2 peroxisomes. No other significant difference between in vivo and in vitro forms of P2 was observed in regards to buoyant density (1.09 g/cm^3 for both forms), size and morphology (Figs. 9, A and B, 10 D), spectra (Fig. 10, A and B), levels (Fig. 10 C) and relative distributions (Fig. 10 E) of matrix and membrane proteins, and phospholipid/protein ratios (Fig. 10 F).

In vitro P3 peroxisomes represent the product of fusion between P1 purified from *pex16-HA* cells and P2 isolated from *pex5KO* cells. In vitro P3 peroxisomes recovered from the fusion reaction after 90 min were very similar to in vivo P3 peroxisomes isolated from wild-type cells in regards to buoyant density (1.14 g/cm^3 for in vitro P3 and 1.15 g/cm^3 for in vivo P3), size and morphology (Figs. 9 and 10 D), spectra of matrix (Fig. 10 A) and membrane (Fig. 10 B) proteins and their relative distributions (Fig. 10 E), levels of matrix and membrane proteins (Fig. 10 C), and phospholipid/protein ratios (Fig. 10 F). In contrast to P2 peroxisomes accumulating mostly (in vivo P2) or only (in vitro P2) pTHI, both the in vivo and in vitro forms of P3 contained exclusively mTHI (Fig. 10 C).

Similar to in vivo P3 purified from wild-type cells, P3 peroxisomes recovered from the in vitro fusion reaction after 90 min were present in four morphologically distinct forms (Fig. 9, C–F). P3-1 appeared as densely staining vesicles, while P3-2 vesicles contained electron-dense material only at their periphery. In P3-3 vesicles, densely staining material was found associated with only some regions of the membrane. In contrast, P3-4 vesicles, which were the most abundant form (Table I, T = 90 min) lacked any internal, densely staining material. None of the four P3 types formed in vitro represents a contaminant, since they were not observed in the preparations of P1 and P2 used for the in vitro fusion reaction (Fig. 9 B). Therefore, the different types of P3 peroxisomes formed in vitro represent the products of fusion of P1 and P2. Importantly, the four morphological types of P3 peroxisomes could also be purified from wild-type cells (Fig. 9, C–F, in vivo) in about the

Table I. Percentage of Different Morphological Types of P3 Peroxisomes

Morphological type	% ± SD		
		In vitro	
	In vivo	T = 10 min	T = 90 min
P3-1	16 ± 4	26 ± 3	13 ± 2
P3-2	15 ± 1	35 ± 4	17 ± 3
P3-3	19 ± 4	28 ± 3	15 ± 3
P3-4	50 ± 8	11 ± 4	55 ± 4

P3 peroxisomes were isolated from YPBO-grown wild-type cells (in vivo) or recovered from the in vitro fusion reaction (in vitro) at 10 and 90 min. Organelles were fixed and processed for EM. Oriented pellet preparations were analyzed. For definition of the morphological types of P3, see text. 300 structures in each of the in vivo and in vitro preparations of P3 were examined.

same distributions as their in vitro counterparts (Table I, compare in vivo to in vitro, T = 90 min). Why there are four distinguishable types of P3 peroxisomes remains obscure. Interestingly, P3 peroxisomes recovered from the in vitro fusion reaction after 10 min contained only 10% as the P3-4 form, while at 90 min ~50% of P3 peroxisomes were of the P3-4 form, similar to the levels found in the in vivo situation (Table I). Based on these data, one could speculate that P3-1, P3-2, P3-3, and P3-4 represent consecutive stages in a post-fusion reorganization of P3 peroxisomes that occurs both in vivo and in vitro.

Taken together, the above data provide evidence that the in vitro fusion of P1 and P2 to yield P3 reconstructs an actual in vivo peroxisome assembly event involving the fusion of distinct small peroxisomal vesicles to form a larger and more dense peroxisomal vesicle.

Discussion

Peroxisome Assembly Pathway

We have previously demonstrated that, based on sedimentation properties, peroxisomes of *Y. lipolytica* belong to two groups, HSP and LSP (Titorenko et al., 1998). In vivo pulse–chase labeling revealed that HSP are precursors to mature LSP peroxisomes (Titorenko et al., 1998). Here, we report the purification of five distinct forms of HSP, designated P1 to P5. LSP are designated P6. In vivo pulse–chase labeling showed that MLS is imported directly from the cytosol with equal efficiency into the matrix of P1 or P2 peroxisomes. In contrast, MLS is not imported into P3, P4, P5, or P6. Therefore, P1 and P2 are import-competent for MLS, while the other peroxisomal subforms are not. In contrast, P2 peroxisomes import two other matrix proteins, AOX and THI, directly from the cytosol, while the other five subforms fail to import these proteins. Our kinetic data on the selective import competencies of distinct peroxisomal subforms are consistent with observed differences in the spectra of matrix and membrane proteins associated with each of the subforms (see Figs. 1–4). Taken together, our data demonstrate that the subforms of HSP differ in their import competencies for various peroxisomal proteins.

Data on the in vivo dynamics of peroxisomal protein localization to distinct HSP subforms show that these subforms are organized into a multistep peroxisome assembly pathway. The pathway operates by conversion of subforms in the direction P1, P2→P3→P4→P5→P6 and involves the import of various peroxisomal proteins into distinct intermediates along the pathway. Several lines of evidence support the physiological basis of this peroxisome assembly pathway. First, as we have presented here, multiple peroxisomal subforms isolated from wild-type cells are not artefactually formed in vitro by fragmentation of LSP or of a singular HSP ancestor during the fractionation procedure. Second, treatment of spheroplasts with sodium azide during pulse–chase experiments is unlikely to cause the formation of (aberrant) peroxisomal forms, as these same forms can be isolated by subcellular fractionation of wild-type cells not treated with azide. Moreover, at different times of chase, pulse-labeled MLS, AOX and THI were localized to different peroxisomal subforms, despite all spheroplasts being treated identically before and after chase (including treatment with azide). Third, the specific order of conversion of different peroxisomal subforms and their selective import competencies have been demonstrated in pulse–chase labeling experiments in vivo using wild-type cells. Fourth, immunofluorescence microscopy has revealed that not >1–2% of all peroxisomes in wild-type cells can be decorated with anti-MLS antibodies, which is a marker protein of all six peroxisomal subforms, but not with anti-SKL antibodies, which is a marker protein of all peroxisomal subforms except P1 and P2 (Titorenko et al., 1998). This low abundance of the two earliest peroxisomal precursors, P1 and P2, is in good agreement with data on the yields of individual forms of HSP and LSP during their purification (see Results).

In the present study we have applied several approaches to provide the first comprehensive experimental evidence for the existence of a multistep peroxisome assembly pathway. Similar pathways have recently been proposed in several models of peroxisome assembly (Subramani, 1996; Erdmann et al., 1997; South and Gould, 1999). These models have been inspired by early data on the heterogeneity of peroxisomes (Heinemann and Just, 1992; Lüers et al., 1993; van Roermund et al., 1995; Wilcke et al., 1995; van der Klei and Veenhuis, 1996), as well as by recent data suggesting a sequential import of membrane and matrix proteins into defined peroxisomal precursors (South and Gould, 1999).

Peroxisome Fusion In Vitro

We have developed an in vitro assay for the fusion of the early peroxisomal subforms, P1 and P2. Fusion of P1 and P2 in vitro was monitored by the extent of proteolytic processing of pTHI to mTHI and was confirmed by purification and EM analysis of docked P1 and P2 and of the P3 form resulting from their fusion.

Homotypic, or self-fusion, is operationally defined as the fusion of vesicles derived from a single organelle, while heterotypic fusion involves fusion between vesicles derived from different organelles (Denesvre and Malhotra, 1996). Homotypic fusion involves identical membranes, while heterotypic fusion occurs between vesicles of different protein composition (Mellman, 1995). Recently, yeast vacuoles have been shown to undergo pseudohetero-

typic fusion in vitro between those vacuoles with only t-SNAREs and those with only v-SNAREs (Ungermann et al., 1998). Despite the fact that in vitro fusion between P1 and P2 involves vesicles from the same compartment type (peroxisome), the protein compositions of the fusion partners are dissimilar (see Figs. 1 and 10). Moreover, neither P1 nor P2 is able to self-fuse in vitro under conditions that support their inter-fusion. Therefore, fusion between P1 and P2 is pseudoheterotypic.

In vitro fusion of P1 and P2 is driven by ATP hydrolysis and requires cytosolic proteins. The intracellular levels and/or the fusogenic activity of these cytosolic proteins are dramatically induced under growth conditions that stimulate extensive peroxisome proliferation. Furthermore, our observation that GTPγS (a nonhydrolyzable analogue of GTP) inhibits peroxisome fusion in vitro suggests the involvement of a Ras-like (Novick and Zerial, 1997) and/or Fzo-like (Hermann and Shaw, 1998) GTPase(s) in the fusion of P1 and P2. In vitro fusion of P1 and P2 also requires Pex1p and Pex6p, two ATPases of the AAA protein family. Organelle biogenesis–associated members of this family contain two AAA cassettes each with an ATP-binding site and are required for all known homotypic and heterotypic membrane fusion reactions (Patel and Latterich, 1998). Our data demonstrate the essential role of Pex1p and Pex6p in the fusion of peroxisomal vesicular structures, which has previously been suggested (Acharya et al., 1995; Faber et al., 1998). Importantly, peroxisome fusion requires two AAA ATPases, similar to the fusion of drug-induced and postmitotic Golgi fragments which is mediated by two other ATPases of the AAA protein family, NSF and p97/VCP (Acharya et al., 1995; Rabouille et al., 1995). In contrast, vacuole fusion (Haas and Wickner, 1996) and fusion of ER membranes (Latterich et al., 1995) in yeast require only one AAA ATPase, Sec18p (NSF), or Cdc48p (p97/VCP), respectively.

The development of an in vitro assay provides a valuable experimental tool for the identification of other components that may be involved in peroxisome fusion, e.g., SNAPs, SNAREs, Ras-, and/or Fzo-like GTPases, and for the elucidation of their roles in the fusion process.

Fusion of P1 and P2 In Vitro Reconstructs an Actual In Vivo Peroxisome Assembly Event

Pulse–chase analysis of the in vivo trafficking of peroxisomal matrix proteins revealed that peroxisomal subform P3 is formed from two earlier subforms, P1 and P2. The results of experiments presented herein support our contention that the in vitro fusion of P1 and P2 to form P3 peroxisomes is a valid reconstruction of an actual biogenetic event involving these subforms during peroxisome assembly in *Y. lipolytica*. First, in vivo P3 peroxisomes isolated from wild-type cells and P3 peroxisomes formed in vitro from the fusion of P1 and P2 peroxisomes contain exclusively mTHI, while P2 peroxisomes accumulate primarily (in vivo) or only (in vitro) pTHI. Second, in vivo P3 isolated from wild-type cells and in vitro P3 peroxisomes recovered from the in vitro fusion reaction are made up of the same four types of vesicular peroxisomal structures. In addition, the percentages of these four types of peroxisomal structures are very similar in the in vivo and in vitro preparations of P3 (Table I, T = 90 min). Third, in vivo and in vitro P3 peroxisomes are very similar according to a number of biochemical criteria including density, matrix and membrane protein spectra and levels, and phospholipid/protein ratio.

That the in vitro fusion of P1 and P2 peroxisomes to make P3 peroxisomes reconstructs an actual early step in peroxisome assembly in vivo is also supported by the fact that the in vitro fusion assay reproduces some genetic requirements of peroxisome biogenesis in vivo. Fusion in vitro requires Pex1p and Pex6p. In vivo, defects in these AAA ATPases affect peroxisome assembly in yeast (Erdmann et al., 1991; Spong and Subramani, 1993; Heyman et al., 1994; Titorenko and Rachubinski, 1998) and in humans (Geisbrecht et al., 1998). Moreover, while inactivation of Pex1p and Pex6p with antibodies affects peroxisome fusion in vitro and prevents formation of the comparatively large (~270 nm) P3 from their smaller (~90 nm) P1 and P2 precursors, *pex1* and *pex6* mutations in vivo prevent the formation of normal peroxisomes and cause the accumulation of small peroxisomal vesicles (Spong and Subramani, 1993; Heyman et al., 1994; Titorenko and Rachubinski, 1998), suggesting a defect in vesicle fusion during peroxisome assembly (Acharya et al., 1995; Faber et al., 1998). Notably, Pex1p and Pex6p have been suggested to form a complex of central importance to peroxisome biogenesis, as disruption of their interaction has been shown to be the most common cause of the peroxisomal biogenesis disorders Zellweger syndrome, neonatal adrenoleukodystrophy, and infantile Refsum disease (Geisbrecht et al., 1998). It should be noted that the role of Pex1p and Pex6p in peroxisome fusion, which has been directly demonstrated in this study and has been suggested by other investigations (Acharya et al., 1995; Erdmann et al., 1997; Faber et al., 1998), is not the only function proposed for these two AAA ATPases. In human cells, Pex1p and Pex6p may also play a role in the stability of Pex5p, the receptor for matrix proteins targeted by peroxisomal targeting signal-1 (Geisbrecht et al., 1998). However, it remains unclear whether the role played by Pex1p and Pex6p in the stability of Pex5p is direct or indirect. The stability and abundance of Pex5p were not decreased in *pex1* and *pex6* mutants of *P. pastoris* (Spong and Subramani, 1993; Heyman et al., 1994; Faber et al., 1998) and *Y. lipolytica* (our unpublished data). For both yeast species, no interaction between Pex1p and Pex5p or between Pex6p and Pex5p has been revealed by yeast two-hybrid analysis (Faber et al., 1998; our unpublished data).

In conclusion, we have demonstrated the existence of a multistep peroxisome assembly pathway in the yeast *Y. lipolytica*. We have also established an in vitro assay that reconstitutes the fusion of two early peroxisomal precursors, and have shown that this in vitro fusion reconstructs an actual early step in peroxisome assembly in vivo. This study provides valuable experimental tools for the identification of other components involved in peroxisome fusion or that are required for the conversion of intermediates of the peroxisome assembly pathway. The identification of such components would not only provide greater insight into the general mechanisms regulating peroxisome assembly in vivo, but would also enhance our understanding of the

molecular defects underlying the peroxisome biogenesis disorders.

We thank Eileen Reklow for help in antisera production.

This work was supported by grant MT-15131 from the Medical Research Council (MRC) of Canada to R.A. Rachubinski. R.A. Rachubinski is an MRC Senior Scientist and an International Research Scholar of the Howard Hughes Medical Institute.

Submitted: 10 September 1999
Revised: 2 December 1999
Accepted: 2 December 1999

References

Acharya, U., R. Jacobs, J.-M. Peters, N. Watson, M.G. Farquhar, and V. Malhotra. 1995. The formation of Golgi stacks from vesiculated Golgi membranes requires two distinct fusion events. *Cell.* 82:895–904.

Aitchison, J.D., R.K. Szilard, W.M. Nuttley, and R.A. Rachubinski. 1992. Antibodies directed against a yeast carboxyl-terminal peroxisomal targeting signal specifically recognize peroxisomal proteins from various yeasts. *Yeast.* 8:721–734.

Banerjee, A., V.A. Barry, B.R. DasGupta, and T.F.J. Martin. 1996. N-ethylmaleimide-sensitive factor acts at a prefusion ATP-dependent step in Ca^{2+}-activated exocytosis. *J. Biol. Chem.* 271:20223–20226.

Bonifacino, J.S., and E.C. Dell'Angelica. 1998. Immunoprecipitation. *In* Current Protocols in Cell Biology. J.S. Bonifacino, M. Dasso, J.B. Harford, J. Lippincott-Schwartz, and K. Yamada, editors. John Wiley and Sons, New York. 7.2.1–7.2.21.

Chamberlain, L.H., D. Roth, A. Morgan, and R.D. Burgoyne. 1995. Distinct effect of α-SNAP, 14-3-3 proteins, and calmodulin on priming and targeting of regulated exocytosis. *J. Cell Biol.* 130:1063–1070.

Denesvre, C., and V. Malhotra. 1996. Membrane fusion in organelle biogenesis. *Curr. Opin. Cell Biol.* 8:519–523.

Erdmann, R., M. Veenhuis, and W.-H. Kunau. 1997. Peroxisomes: organelles at the crossroads. *Trends Cell Biol.* 7:400–407.

Erdmann, R., F.F. Wiebel, A. Flessau, J. Rytka, A. Beyer, K.-U. Fröhlich, and W.-H. Kunau. 1991. *PAS1*, a yeast gene required for peroxisome biogenesis, encodes a member of a novel family of putative ATPases. *Cell.* 64:499–510.

Eitzen, G.A., R.K. Szilard, and R.A. Rachubinski. 1997. Enlarged peroxisomes are present in oleic acid-grown *Yarrowia lipolytica* overexpressing the *PEX16* gene encoding an intraperoxisomal peripheral membrane peroxin. *J. Cell Biol.* 137:1265–1278.

Eitzen, G.A., V.I. Titorenko, J.J. Smith, M. Veenhuis, R.K. Szilard, and R.A. Rachubinski. 1996. The *Yarrowia lipolytica* gene *PAY5* encodes a peroxisomal integral membrane protein homologous to the mammalian peroxisome assembly factor PAF-1. *J. Biol. Chem.* 271:20300–20306.

Faber, K.N., J.A. Heyman, and S. Subramani. 1998. Two AAA family peroxins, PpPex1p and PpPex6p, interact with each other in an ATP-dependent manner and are associated with different subcellular membranous structures distinct from peroxisomes. *Mol. Cell. Biol.* 18:936–943.

Geisbrecht, B.V., C.S. Collins, B.E. Reuber, and S.J. Gould. 1998. Disruption of a PEX1-PEX6 interaction is the most common cause of the neurologic disorders Zellweger syndrome, neonatal adrenoleukodystrophy, and infantile Refsum disease. *Proc. Natl. Acad. Sci. USA.* 95:8630–8635.

Haas, A., and W. Wickner. 1996. Homotypic vacuole fusion requires Sec17p (yeast α-SNAP) and Sec18p (yeast NSF). *EMBO (Eur. Mol. Biol. Organ.) J.* 15:3296–3305.

Heinemann, P., and W.W. Just. 1992. Peroxisomal protein import. In vivo evidence for a novel translocation competent compartment. *FEBS Lett.* 300: 179–182.

Hermann, G.J., and J.M. Shaw. 1998. Mitochondrial dynamics in yeast. *Annu. Rev. Cell Dev. Biol.* 14:265–303.

Heyman, J.A., E. Monosov, and S. Subramani. 1994. Role of the *PAS1* gene of *Pichia pastoris* in peroxisome biogenesis. *J. Cell Biol.* 127:1259–1273.

Latterich, M., K.-U. Fröhlich, and R. Schekman. 1995. Membrane fusion and the cell cycle: Cdc48p participates in the fusion of ER membranes. *Cell.* 82: 885–893.

Latterich, M., and R. Schekman. 1994. The karyogamy gene KAR2 and novel proteins are required for ER-membrane fusion. *Cell.* 78:87–98.

Lüers, G., T. Hashimoto, H.D. Fahimi, and A. Völkl. 1993. Biogenesis of peroxisomes: isolation and characterization of two distinct peroxisomal populations from normal and regenerating rat liver. *J. Cell Biol.* 121:1271–1280.

Matsuoka, K., D.C. Bassham, N.V. Raikhel, and K. Nakamura. 1995. Different sensitivity to wortmannin of two vacuolar sorting signals indicates the presence of distinct sorting machineries in tobacco cells. *J. Cell Biol.* 130:1307–1318.

Mellman, I. 1995. Enigma variations: protein mediators of membrane fusion. *Cell.* 82:869–872.

Nichols, B.J., C. Ungermann, H.R.B. Pelham, W. Wickner, and A. Haas. 1997. Homotypic vacuolar fusion mediated by t- and v-SNAREs. *Nature.* 387: 199–202.

Novick, P., and M. Zerial. 1997. The diversity of Rab proteins in vesicle transport. *Curr. Opin. Cell Biol.* 9:496–504.

Otto, H., P.I. Hanson, and R. Jahn. 1997. Assembly and disassembly of a ternary complex of synaptobrevin, syntaxin, and SNAP-25 in the membrane of synaptic vesicles. *Proc. Natl. Acad. Sci. USA.* 94:6197–6201.

Patel, S., and M. Latterich. 1998. The AAA team: related ATPases with diverse functions. *Trends Cell Biol.* 8:65–71.

Pfeffer, S.R. 1996. Transport vesicle docking: SNAREs and associates. *Annu. Rev. Cell Dev. Biol.* 12: 441–461.

Purdue, P.E., and P.B. Lazarow. 1995. Identification of peroxisomal membrane ghosts with an epitope-tagged integral membrane protein in yeast mutants lacking peroxisomes. *Yeast.* 11:1045–1060.

Rabouille, C., T.P. Levine, J.-M. Peters, and G. Warren. 1995. An NSF-like ATPase, p97, and NSF mediate cisternal regrowth from mitotic Golgi fragments. *Cell.* 82:905–914.

Rexach, M.F., and R.W. Schekman. 1991. Distinct biochemical requirements for the budding, targeting, and fusion of ER-derived transport vesicles. *J. Cell Biol.* 114:219–229.

Roggenkamp, R., H. Sahm, W. Hinkelmann, and F. Wagner. 1975. Alcohol oxidase and catalase in peroxisomes of methanol-grown *Candida boidinii*. *Eur. J. Biochem.* 59:231–236.

Rothman, J.E. 1994. Mechanisms of intracellular protein transport. *Nature.* 372: 55–63.

Rothman, J.E., and G. Warren. 1994. Implications of the SNARE hypothesis for intracellular membrane topology and dynamics. *Curr. Biol.* 4:220–233.

South, S.T., and S.J. Gould. 1999. Peroxisome synthesis in the absence of preexisting peroxisomes. *J. Cell Biol.* 144:255–266.

Spong, A.P., and S. Subramani. 1993. Cloning and characterization of *PAS5*: a gene required for peroxisome biogenesis in the methylotrophic yeast *Pichia pastoris*. *J. Cell Biol.* 123:535–548.

Subramani, S. 1996. Protein translocation into peroxisomes. *J. Biol. Chem.* 271: 32483–32486.

Szilard, R.K., V.I. Titorenko, M. Veenhuis, and R.A. Rachubinski. 1995. Pay32p of the yeast *Yarrowia lipolytica* is an intraperoxisomal component of the matrix protein translocation machinery. *J. Cell Biol.* 131:1453–1469.

Tamura, S., K. Okumoto, R. Toyama, N. Shimozawa, T. Tsukamoto, Y. Suzuki, T. Osumi, N. Kondo, and Y. Fujiki. 1998. Human *PEX1* cloned by functional complementation on a CHO cell mutant is responsible for peroxisome-deficient Zellweger syndrome of complementation group I. *Proc. Natl. Acad. Sci. USA.* 95:4350–4355.

Titorenko, V.I., G.A. Eitzen, and R.A. Rachubinski. 1996. Mutations in the *PAY5* gene of the yeast *Yarrowia lipolytica* cause the accumulation of multiple subforms of peroxisomes. *J. Biol. Chem.* 271:20307–20314.

Titorenko, V.I., D.M. Ogrydziak, and R.A. Rachubinski. 1997. Four distinct secretory pathways serve protein secretion, cell surface growth, and peroxisome biogenesis in the yeast *Yarrowia lipolytica*. *Mol. Cell. Biol.* 17:5210–5226.

Titorenko, V.I., and R.A. Rachubinski. 1998. Mutants of the yeast *Yarrowia lipolytica* defective in protein exit from the endoplasmic reticulum are also defective in peroxisome biogenesis. *Mol. Cell. Biol.* 18:2789–2803.

Titorenko, V.I., J.J. Smith, R.K. Szilard, and R.A. Rachubinski. 1998. Pex20p of the yeast *Yarrowia lipolytica* is required for the oligomerization of thiolase in the cytosol and for its targeting to the peroxisome. *J. Cell Biol.* 142:403–420.

Ungermann, C., B.J. Nichols, H.R.B. Pelham, and W. Wickner. 1998. A vacuolar v-t-SNARE complex, the predominant form in vivo and on isolated vacuoles, is disassembled and activated for docking and fusion. *J. Cell Biol.* 140: 61–69.

Ungermann, C., and W. Wickner. 1998. Vam7p, a vacuolar SNAP-25 homolog, is required for SNARE complex integrity and vacuole docking and fusion. *EMBO (Eur. Mol. Biol. Organ.) J.* 17:3269–3276.

van der Klei, I.J., and M. Veenhuis. 1996. Peroxisome biogenesis in the yeast *Hansenula polymorpha*: a structural and functional analysis. *Ann. NY Acad. Sci.* 804:47–59.

van Roermund, C.W.T., M. van der Berg, and R.J.A. Wanders. 1995. Localization of peroxisomal 3-oxoacyl-CoA thiolase in particles of varied density in rat liver: implications for peroxisome biogenesis. *Biochim. Biophys. Acta.* 1245:348–358.

Wang, H.J., M.-T. Le Dall, Y. Waché, C. Laroche, J.-M. Belin, C. Gaillardin, and J.-M. Nicaud. 1999. Evaluation of acyl coenzyme A oxidase (Aox) isozyme function in the n-alkane-assimilating yeast. *Yarrowia lipolytica. J. Bacteriol.* 181:5140–5148.

Warren, G., and W. Wickner. 1996. Organelle inheritance. *Cell.* 84:395–400.

Weber, T., B.V. Zemelman, J.A. McNew, B. Westermann, M. Gmachl, F. Parlati, T.H. Söllner, and J.E. Rothman. 1998. SNAREpins: minimal machinery for membrane fusion. *Cell.* 92:759–772.

Wilcke, M., K. Hultenby, and S.E.H. Alexson. 1995. Novel peroxisomal populations in subcellular fractions from rat liver. Implications for peroxisome structure and biogenesis. *J. Biol. Chem.* 270:6949–6958.

Xu, Z., K. Sato, and W. Wickner. 1998. LMA1 binds to vacuoles at Sec18p (NSF), transfers upon ATP hydrolysis to a t-SNARE (Vam3p) complex, and is released during fusion. *Cell.* 93:1125–1134.